O-GlcNAcylation Increases ChREBP Protein Content and Transcriptional Activity in the Liver

Céline Guinez,[1,2,3] Gaëlle Filhoulaud,[1,2,3] Fadila Rayah-Benhamed,[1,2,3] Solenne Marmier,[1,2,3] Céline Dubuquoy,[1,2,3] Renaud Dentin,[1,2,3] Marthe Moldes,[1,2,3] Anne-Françoise Burnol,[1,2,3] Xiaoyong Yang,[4] Tony Lefebvre,[5] Jean Girard,[1,2,3] and Catherine Postic[1,2,3]

OBJECTIVE—Carbohydrate-responsive element–binding protein (ChREBP) is a key transcription factor that mediates the effects of glucose on glycolytic and lipogenic genes in the liver. We have previously reported that liver-specific inhibition of ChREBP prevents hepatic steatosis in ob/ob mice by specifically decreasing lipogenic rates in vivo. To better understand the regulation of ChREBP activity in the liver, we investigated the implication of O-linked β-N-acetylglucosamine (O-GlcNAc or O-GlcNAcylation), an important glucose-dependent posttranslational modification playing multiple roles in transcription, protein stabilization, nuclear localization, and signal transduction.

RESEARCH DESIGN AND METHODS—O-GlcNAcylation is highly dynamic through the action of two enzymes: the O-GlcNAc transferase (OGT), which transfers the monosaccharide to serine/threonine residues on a target protein, and the O-GlcNAcase (OGA), which hydrolyses the sugar. To modulate ChREBP^{OG} in vitro and in vivo, the OGT and OGA enzymes were overexpressed or inhibited via adenoviral approaches in mouse hepatocytes and in the liver of C57BL/6J or obese db/db mice.

RESULTS—Our study shows that ChREBP interacts with OGT and is subjected to O-GlcNAcylation in liver cells. O-GlcNAcylation stabilizes the ChREBP protein and increases its transcriptional activity toward its target glycolytic (L-PK) and lipogenic genes (ACC, FAS, and SCD1) when combined with an active glucose flux in vivo. Indeed, OGT overexpression significantly increased ChREBP^{OG} in liver nuclear extracts from fed C57BL/6J mice, leading in turn to enhanced lipogenic gene expression and to excessive hepatic triglyceride deposition. In the livers of hyperglycemic obese db/db mice, ChREBP^{OG} levels were elevated compared with controls. Interestingly, reducing ChREBP^{OG} levels via OGA overexpression decreased lipogenic protein content (ACC, FAS), prevented hepatic steatosis, and improved the lipidic profile of OGA-treated db/db mice.

CONCLUSIONS—Taken together, our results reveal that O-GlcNAcylation represents an important novel regulation of ChREBP activity in the liver under both physiological and pathophysiological conditions. *Diabetes* 60:1399–1413, 2011

The liver is responsible for the conversion of excess dietary carbohydrates into triglycerides (TGs) through de novo lipogenesis. Appropriate control of this pathway is crucial because excess fatty acids lead to hepatic steatosis and to related metabolic diseases such as insulin resistance and type 2 diabetes (1). In recent years, studies reported that liver transcription factor carbohydrate-responsive element–binding protein (ChREBP) is required for the induction of the glycolytic enzyme L-pyruvate kinase (L-PK) by glucose, and that acting in synergy with sterol regulatory element–binding protein (SREBP)-1c, ChREBP is necessary for the induction of lipogenic genes (acetyl-CoA carboxylase [ACC] and fatty acid synthase [FAS]) in response to glucose and insulin (2–4). Importantly, liver-specific inhibition of ChREBP, by decreasing lipogenic rates, improves hepatic steatosis and insulin resistance in obese ob/ob mice (5,6). Therefore, ChREBP could be a potential therapeutic target, and an accurate knowledge of the mechanisms regulating its activity is crucial for the development of pharmacological approaches for the treatment of metabolic diseases.

Under low glucose concentrations, ChREBP, which is phosphorylated on serine-196 (Ser-196) and threonine-666 (Thr-666) residues, is cytosolic and inactive (7). When glucose concentrations rise, ChREBP undergoes a first dephosphorylation on Ser-196, allowing its nuclear translocation, and a second on Thr-666, leading to the activation of its target genes through the binding on the carbohydrate responsive element (ChoRE) (7). We demonstrated the relevance of modulating Ser-196 phosphorylation for ChREBP intracellular localization in response to glucose and/or glucagon (8). However, the fact that mutations of Ser-196 and/or Thr-666 do not result in a constitutively active form of ChREBP (9) suggests that additional glucose-dependent posttranslational modifications may be involved in ChREBP activation.

Key transcription factors are modified by O-linked β-N-acetylglucosamine (O-GlcNAcylation or O-GlcNAc) in the liver (10–15). The discovery that FoxO1 and cAMP-responsive element–binding protein (CREB)–regulated transcription coactivator 2 (CRTC2), both involved in the transcriptional regulation of gluconeogenesis (16,17), are O-GlcNAcylated provided a novel mechanism by which hyperglycemia reinforces hepatic glucose production and worsens glucose intolerance (11,12,18). O-GlcNAcylation is highly dynamic through the action of two enzymes: the O-GlcNAc transferase (OGT), which transfers the monosaccharide to serine/threonine residues on a target protein, and the O-GlcNAcase (OGA), which hydrolyses the sugar (19) (Fig. 1A). O-GlcNAcylation can modulate protein
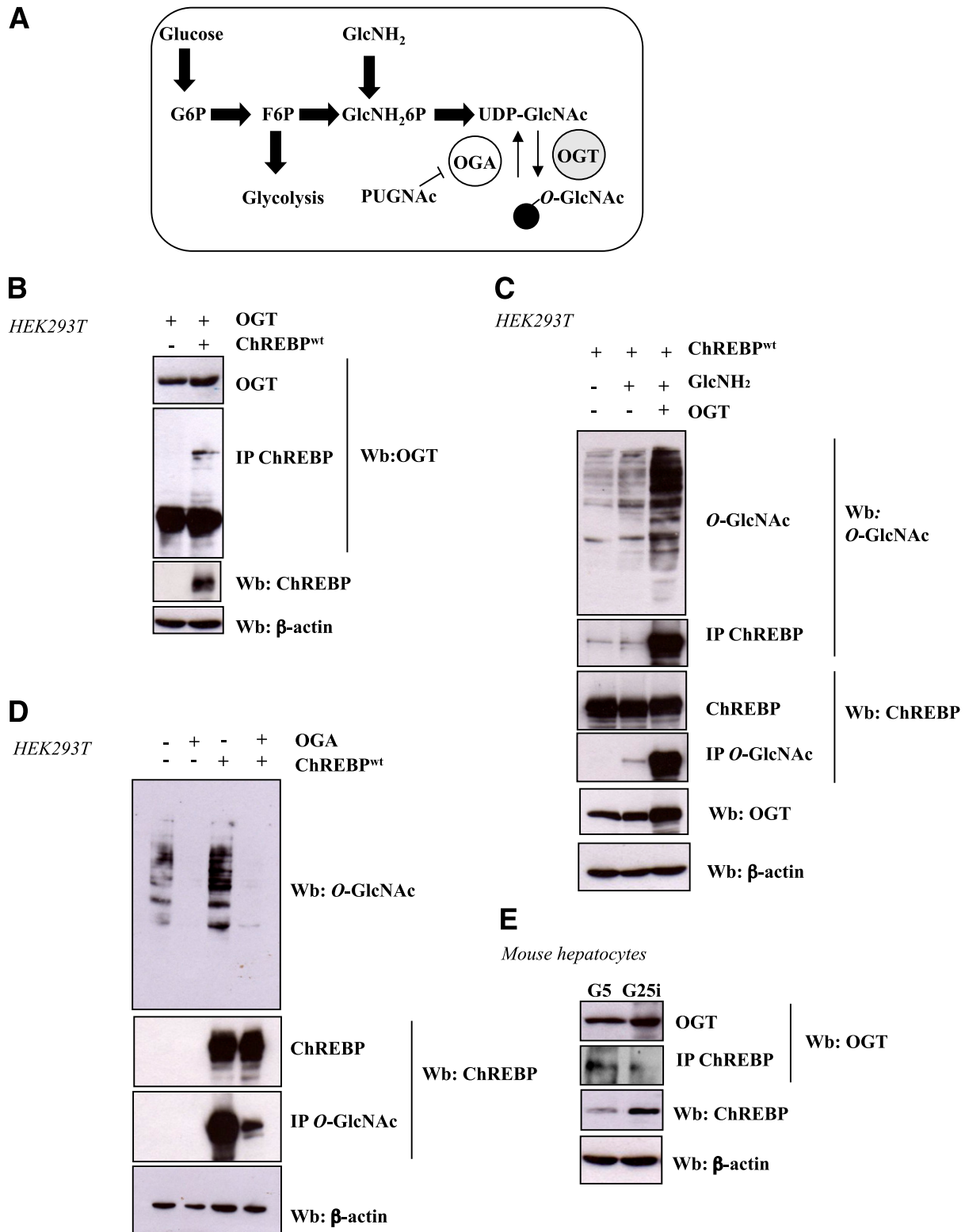
FIG. 1. ChREBP interacts with OGT and is *O*-GlcNAcylated in a dynamic manner in HEK293T cells and in mouse hepatocytes. *A*: Schematic diagram of the UDP-GlcNAc pathway. *O*-GlcNAcylation is an important posttranslational modification that has been proposed to be a nutrient sensor because the donor sugar, UDP-GlcNAc, receives input from multiple metabolic pathways. Activity of OGT, the enzyme that transfers the monosaccharide to serine/threonine residues, depends upon UDP-GlcNAc concentrations. Of glucose that enters the cells, 2–5% is used for production of the donor sugar nucleotide. The addition of GlcNH$_2$ directly enters the hexosamine biosynthetic pathway. PUGNAc is an inhibitor of the OGA that hydrolyses the sugar. *B*: HEK239T cells were cotransfected with OGT (1 µg) and ChREBP^{wt} plasmids (1 µg) and incubated for 24 h under high glucose conditions (G25). Immunoprecipitation (IP) of ChREBP was analyzed by immunoblotting with an OGT antibody. β-Actin was used as loading control. Representative Western blots (Wb) are shown. $n = 3$ independent experiments. *C*: ChREBP-overexpressing HEK293T cells were incubated under low glucose medium plus 5 mM GlcNH$_2$ or transfected with an OGT-expressing vector or both. Representative Western blots are shown. $n = 3$ independent experiments. *D*: Overexpression of OGA (1 µg) in HEK293T cells cultured in 25 mM glucose leads to a decrease in global and transfected ChREBP^{OG}. Representative Western blots are shown. $n = 3$ independent experiments. *E*: Immunoprecipitated ChREBP from primary mouse hepatocytes incubated for 24 h in either low glucose (G5) or high glucose plus insulin (G25i) was immunoblotted with an OGT

stability, cellular localization, activity, and partner interactions (20–22). O-GlcNAcylation acts as a nutrient sensor, since the intracellular concentration of the donor sugar for O-GlcNAcylation, uridine diphosphate GlcNAc, rapidly responds to flux through multiple metabolic pathways. O-GlcNAcylation is the end product of the hexosamine biosynthetic pathway (Fig. 1A), a metabolic pathway that has emerged as a major determinant of metabolic disorders associated with insulin resistance and/or type 2-diabetes (10,23,24).

In the current study, we report that O-GlcNAcylation, by stabilizing the ChREBP protein and stimulating its transcriptional activity, increases ChREBP activity under hyperglycemic conditions in the liver. In addition, we show that modulation of ChREBP O-GlcNAcylation (ChREBP^{OG}) through the activities of OGT and/or OGA enzymes is an important determinant of fatty acid synthesis in the mouse liver.

RESEARCH DESIGN AND METHODS

Six- to 12-week-old male C57BL/6J and db/db mice were purchased from Elevage Janvier. Procedures were carried out according to the French guidelines for the care of experimental animals. Mice were adapted to the environment for 1 week prior to study and maintained in a 12-h light/dark cycle with water and regular diet (65% carbohydrate, 11% fat, and 24% protein). Green fluorescent protein (GFP) (Laboratoire de Thérapie Génique, Nantes, France), OGT (11), and OGA (24) adenovirus were delivered by penis vein injection (5×10^9 plaque-forming units [pfu]/mouse). Seven days after OGT injection, mice were fasted for 24 h or refed on a regular diet for 18 h. For OGA studies, mice were killed in the fed state 10 days after adenoviral injection. For gavage experiments, 24-h fasted mice received glucosamine (GlcNH$_2$, 2.5 g/kg) or glucose (5 g/kg) orally and were killed 4, 8, or 12 h later. Mice were killed after an intraperitoneal anesthesia (a ketamine/xylazine mix). Livers were flash-frozen and stored at –80°C.

Glucose and insulin tolerance tests. Glucose tolerance tests were performed by glucose gavage (1 g D-glucose/kg body wt) after an overnight fast. Insulin tolerance tests were performed by intraperitoneal injection of human regular insulin (0.75 unit insulin/kg body wt, Actrapid Penfill; NovoNordisk) 5 h after food removal. Blood glucose was determined using one-touch Accu-Check glucometer (Roche).

Primary cultures of hepatocytes. Hepatocytes were isolated and cultured as described (2). Hepatocytes were incubated under low glucose concentrations (G5) for 24 h and then infected with specific adenovirus (5 pfu/cell: GFP, OGT (11), OGA (24), short hairpin RNA [shRNA] ChREBP [shChREBP; Genecust] or shRNAOGT [shOGT, Genecust]) for 5 h. Cells were then cultured in the presence of low (5 mmol/L [G5]) or high (25 mmol/L [G25]) glucose and insulin concentrations (100 nM) (G25i) for 24 h. For protein stability experiments, hepatocytes were incubated in G5 or in G25i for 24 h. Cells were then incubated with G5, G25i, or 5 mmol/L GlcNH$_2$ for 8 h. Simultaneously added were 8 μM of MG132 (a proteasome inhibitor [N-carbobenzoxyl-Leu-Leu-leucinal, 8 mmol/L stock solution in DMSO, Sigma]) or DMSO.

Transfections in HEK293T cells. Human embryonic kidney cells (HEK293T) were grown in 25 mM D-glucose Dulbecco's modified Eagle's medium supplemented with 10% fetal calf serum. OGT, OGA (11), wild-type ChREBP (ChREBP^{wt}), and the dephosphorylated ChREBP isoform (ChREBP^{DP}, mutated on Ser-196 and Thr-666 residues [4]) plasmids were previously described. Using lipofectamine 2000 (Invitrogen), 1 μg of plasmid was transfected in HEK293T cells according to the manufacturer. Cells were then incubated in G25 or G25i and/or 5 mmol/L GlcNH$_2$. For ubiquitynilation experiments, HEK293T cells were cotransfected with 1 μg of ChREBP^{wt} and with an ubiquitin hemagglutinin (HA)-tagged plasmid. Cells were incubated in G25 for 24 h. MG132 (20 μM) or DMSO were added for 7 h. ChREBP immunoprecipitates were immunoblotted with HA antibodies to detect ubiquitinylated forms of ChREBP.

Luciferase reporter assays. HepG2 hepatoma cells were grown in 25 mM D-glucose Dulbecco's modified Eagle's medium supplemented with 10% fetal calf serum and were transfected using 250 ng of a L-PK luciferase reporter construct containing three ChoRE sequences as previously described or an empty PGL-3 luciferase construct for control (25). Cotransfections were performed using 250 ng of ChREBP^{wt} and 250 ng of β-galactosidase plasmid for normalization. At 24 h posttransfection, cells were incubated with glucose or PUGNAc for 4 h, and luciferase assay was performed after cell lysis. β-Galactosidase assays were performed for normalization of ChoRE-luciferase activity.

Immunoprecipitation and wheat germ agglutinin purification. For O-GlcNAc protein immunoprecipitation, cells were lysed on ice with radio-immunoprecipitation (RipA) buffer (10 mmol/L Tris/HCl, 150 mmol/L NaCl, 1% Triton X-100 [v/v], 0.5% sodium deoxycholate [w/v], 0.1% sodium dodecyl sulfate [w/v], and protease inhibitors; pH 7.4). For ChREBP immunoprecipitation, cells were lysed on ice with IPH buffer (20 mmol/L Tris/HCl, 150 mmol/L NaCl, 0.5% NP-40 [v/v], and protease inhibitors; pH 8.0). Cellular extracts were then centrifuged at 20,000g for 10 min at 4°C. Supernatants were incubated with 3 μL of the mouse monoclonal anti–O-GlcNAc antibody (RL2, Affinity Bioreagents) or 3 μL of the rabbit polyclonal anti-ChREBP antibody and placed at 4°C overnight. Bound proteins were recovered after addition of 30 μL of Sepharose-labeled protein G (Sigma) or A (Invitrogen) for 1 h at 4°C. Beads were gently centrifuged for 1 min and washed with the following buffers for O-GlcNAc protein immunoprecipitation: RipA buffer, RipA supplemented with 500 mmol/L NaCl and TNE (10 mmol/L Tris/HCl, 150 mmol/L NaCl, and 1mM EDTA; pH 7.4) in equal volume, and finally with TNE alone or with IPH buffer for other specific immunoprecipitation. For coimmunoprecipitation, cells were lysed on ice in the smooth IPH buffer. Whole cell extracts were centrifuged at 20,000g for 10 min at 4°C, and supernatants were collected. Three microliters of the anti-ChREBP antibody were added to the supernatants overnight at 4°C, followed by an incubation with Sepharose-labeled protein A for 1 h at 4°C. Beads were gently centrifuged for 1 min and washed four times for 5 min each with the smooth lysis buffer. Bound proteins were analyzed by Western blot with a polyclonal anti-OGT antibody (1:5000, Sigma).

For wheat germ agglutinin ([WGA] a specific GlcNAc lectin) precipitation, cells were lysed with RipA buffer supplemented or not with 0.5 M of GlcNAc (Sigma) and extracts (1 mg of proteins) were incubated with 30 μl of WGA agarose beads (Sigma) with or without 0.5M GlcNAc for 2 h at 4°C. After three washes (with or without 0.5M GlcNAc), proteins were eluted from the beads in 2× Laemmli buffer and separated by SDS-PAGE.

Chromatin immunoprecipitation. Chromatin immunoprecipitation (ChIP) assays were performed as previously described (11). Proteins were cross-linked to DNA by addition of 1% formaldehyde to the fresh liver following incubation for 15 min at 37°C. Sonication was performed by 15 10-s pulses. Immunoprecipitation was performed with a ChREBP antibody (NB400–135; Novus Biologicals). Immune complexes were captured with 50 μl of 50% Protein G agarose/salmon sperm DNA (Upstate). DNA fragments were quantified by real-time PCR. L-PK promoter primers were as follows: forward, 5′-GTCCCACACTTTGGAAGCAT-3′ and reverse, 5′-CCCAACACTGATTCTACCC-3′.

Gene expression analysis. Total cellular RNAs were extracted using the RNeasy Kit (Promega) (2). Primers used for cyclophilin, ChREBP, L-PK, ACC, FAS, SCD1, SREBP-1, and OGA were previously described (2,8,24). Primers used for OGT were as follows: sense, 5′-TCGCACAGCTCTGTCAAAAA-3′and antisense, 5′-GCCCTGGGTCGCTTGGAAGA-3′. The relative quantification for a given gene was corrected to the cyclophilin mRNA values.

Liver extracts and immunoblot analysis. Nuclear and cytoplasmic extracts were prepared using the NE-PER extraction reagent kit (Pierce Biotechnology). Liver proteins (80 μg) were subjected to SDS-PAGE analysis. ChREBP (Novus Biologicals), SREBP-1c (Interchim), ACC antibody (Cell Signaling), and OGT (DM17; Sigma) were detected with polyclonal antibodies. The FAS antibody was a gift from I. Dugail (Centre de Recherche des Cordeliers, Paris, France). The CRTC2 antibody was used as described (11). β-Actin (Sigma-Aldrich), GAPDH, and lamin A/C antibodies were used as loading controls. ChREBP immunohistochemistry was performed as described (8).

Metabolic analysis. Glucose-6-phosphate (G6P) concentrations were determined as described (2). Liver TG was measured with a colorimetric diagnostic kit (Triglycerides FS; Diasys). Plasma TG and nonesterified fatty acids were determined using an automated Monarch device (Bichat, Paris). Serum insulin concentrations were determined using a rat insulin ELISA assay kit (Crystal Chem) with a mouse insulin standard.

Staining techniques. For detection of neutral lipids, mouse hepatocytes and liver cryosections were fixed and stained with the Oil Red O technique (26) using 0.23% dye dissolved in 65% isopropyl alcohol for 10 min.

Statistical analyses. The results are expressed as means ± SEM. Statistical significance was assessed using the ANOVA test (StatView). Differences were considered statistically significant at P < 0.05.

---

antibody in order to evaluate the interaction between the two endogenous proteins. β-Actin was used as a loading control. Representative Western blots are shown. n = 3 independent experiments. (A high-quality color representation of this figure is available in the online issue.)
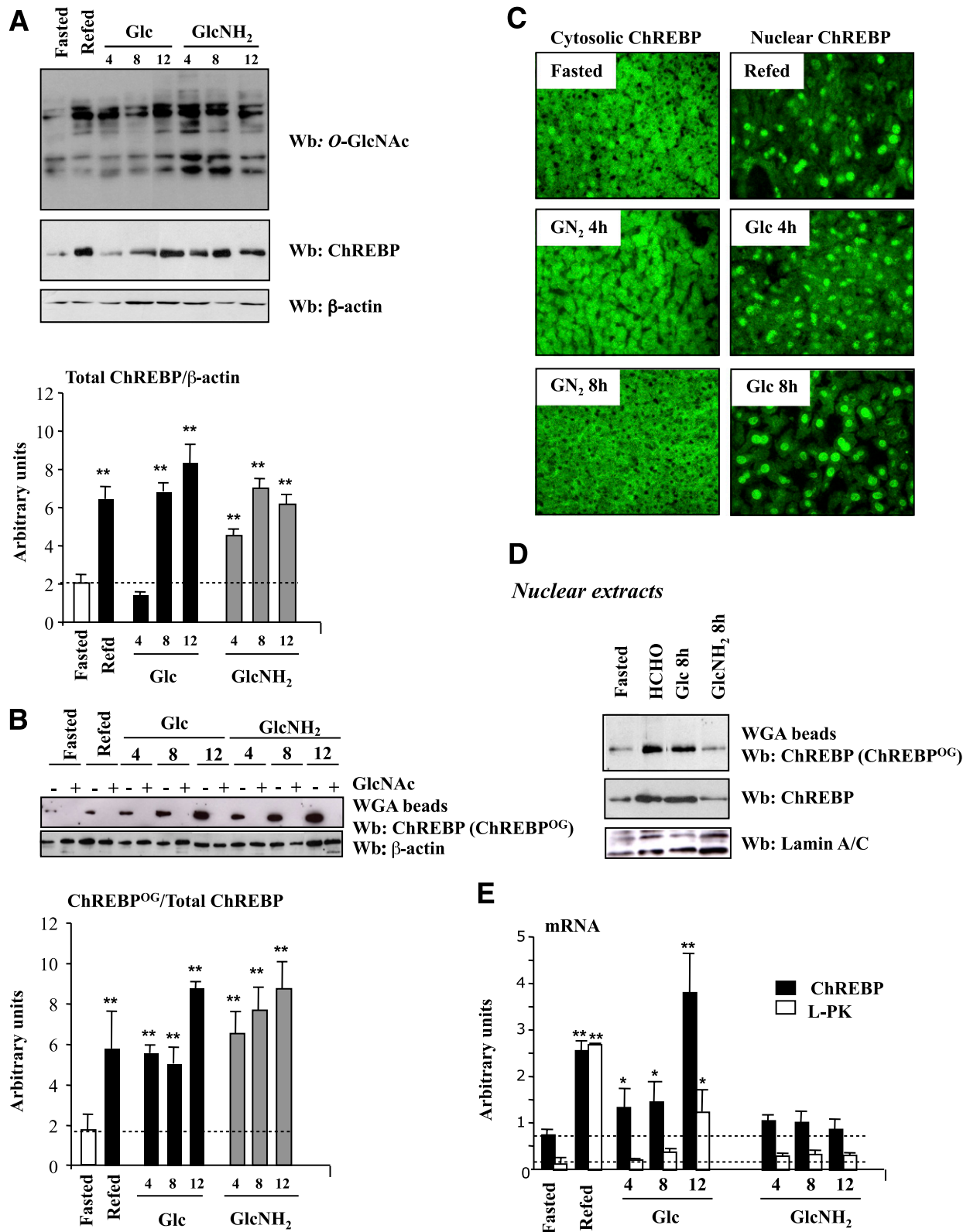
A

Wb: *O*-GlcNAc

Wb: ChREBP

Wb: β-actin

Total ChREBP/β-actin

B

GlcNAc
WGA beads
Wb: ChREBP (ChREBP^{OG})
Wb: β-actin

ChREBP^{OG}/Total ChREBP

C

Cytosolic ChREBP   Nuclear ChREBP

D

Nuclear extracts

WGA beads
Wb: ChREBP (ChREBP^{OG})

Wb: ChREBP

Wb: Lamin A/C

E

mRNA

■ ChREBP
□ L-PK

FIG. 2. **Elevated *O*-GlcNAc levels by GlcNH$_2$ administration in vivo increases ChREBP protein content.** Four groups of C57BL/6J mice were studied: a 24-h fasted group, a fasted group refed a regular diet for 18 h, and the last groups of mice were force-fed with glucose (5 g/kg) or GlcNH$_2$ (2.5 g/kg) after the fasting period. Mice were killed at the indicated time and livers were analyzed. *A*: Western blot (Wb) analysis of *O*-GlcNAc and ChREBP levels. β-Actin was used as a loading control. Lanes were run on the same gel but were noncontiguous. Representative Western blots are shown. Quantification of the ratio of total ChREBP compared with β-actin content is shown. Data are means ± SEM. *n* = 6–10 per group. **P < 0.005 compared with the fasting state. *B*: ChREBP^{OG} was evaluated by purification of proteins with an *O*-GlcNAc–specific lectin, WGA. Specificity of the binding was confirmed by GlcNAc (0.5 M) competition. A representative Western blot is shown. β-Actin was used as a loading control. Quantification of the ratio of ChREBP^{OG} compared with total ChREBP content is shown. Data are means ± SEM. *n* = 6–10 per group. **P < 0.005 compared with the fasting state. *C*: Immunofluorescence analysis of ChREBP in liver sections from 24-h fasted, refed, and force-fed mice with either glucose (5 g/kg) or GlcNH$_2$ (2.5 g/kg) after the fasting period. No signal was obtained when liver sections were incubated with the secondary antibody only (data not

RESULTS

ChREBP interacts with OGT and is *O*-GlcNAcylated in HEK293T cells and in hepatocytes. We first examined whether ChREBP interacted with OGT and could be modified by *O*-GlcNAcylation (Fig. 1). The interaction between ChREBP and OGT was detected in HEK293T cells after cotransfection with OGT (11) and ChREBP^{wt} (27) (Fig. 1*B*). To demonstrate that OGT interaction with ChREBP leads to its *O*-GlcNAcylation, HEK293T cells were cotransfected with OGT and ChREBP^{wt} (Fig. 1*C*). Global *O*-GlcNAcylation levels were enhanced by the addition of 5 mmol/L GlcNH$_2$, which enters the hexosamine biosynthetic pathway downstream of the limiting step (Fig. 1*A*). Immunoprecipitated ChREBP was immunoblotted with an anti–*O*-GlcNAc antibody, or conversely, immunoprecipitated *O*-GlcNAcylated proteins were immunoblotted with an anti-ChREBP antibody (Fig. 1*C*). ChREBP was highly *O*-GlcNAcylated under GlcNH$_2$ plus OGT conditions (Fig. 1*C*). ChREBP^{OG} is a dynamic process, since overexpression of OGA, the enzyme responsible for global deglycosylation of proteins, markedly decreased ChREBP^{OG} in HEK293T cells (Fig. 1*D*).

We tested whether an interaction between ChREBP and OGT also occurred in mouse hepatocytes (Fig. 1*E*). Hepatocytes were cultured under low (G5) or high glucose plus insulin (G25i) for 24 h. OGT was copurified in ChREBP immunoprecipitates, thereby revealing a direct interaction between the two proteins. Interestingly, the interaction between ChREBP and OGT was stronger under low glucose concentrations (Fig. 1*E*).

GlcNH$_2$ administration in vivo increases ChREBP protein concentrations in the liver. To investigate the effect of *O*-GlcNAcylation on ChREBP expression and/or activity, nutritional studies were performed in vivo (Fig. 2). Mice were fasted for 24 h and were then either refed for 18 h on a regular diet, or force-fed with glucose (5 g/kg) or GlcNH$_2$ (2.5 g/kg).

Under fasting conditions, blood glucose and G6P concentrations were low (Supplementary Fig. 1), and as a consequence, ChREBP protein content and mRNA levels remain low (Figs. 2*A* and 2*E*). Low global glycosylation levels (Fig. 2*A*) and ChREBP^{OG} revealed by WGA were detected in parallel. Incubation of lysates with 0.5 M free GlcNAc revealed the specificity of the binding (Fig. 2*B*). Under fasting conditions, ChREBP was cytosolic (Fig. 2*C*), and as a result, ChREBP target gene *L-PK* was not induced (Fig. 2*E*).

Under refed and glucose gavage conditions (all times examined), blood glucose and hepatic G6P concentrations were significantly increased above fasting values (Supplementary Fig. 1). Global and ChREBP^{OG} levels were increased compared with fasting conditions (Figs. 2*A* and 2*B*). Under glucose gavage conditions, ChREBP protein content was gradually increased over 12 h (Fig. 2*A*) because of a time-dependent increase in mRNA levels (Fig. 2*E*). It should be noted, however, that the induction of the *L-PK* gene occurred 12 h after the beginning of the glucose gavage—and this despite the presence of nuclear ChREBP as early as 4 h (Fig. 2*C* and 2*E*).

As soon as 4 h of GlcNH$_2$ gavage, ChREBP protein content was significantly increased compared with both fasting and glucose gavage conditions (Fig. 2*A*). After 8 h, equivalent protein content was reached and was maintained up to 12 h after the starting time point of the gavages (glucose and GlcNH$_2$) (Fig. 2*A*). ChREBP^{OG} followed a similar pattern (Fig. 2*B*). In contrast to glucose, the GlcNH$_2$-mediated induction of ChREBP was not associated with increased mRNA content (Fig. 2*E*). Because blood glucose and G6P concentrations were not increased above fasting values during the course of the GlcNH$_2$ gavage (Supplementary Fig. 1), ChREBP remained cytosolic (Fig. 2*C*). Nuclear ChREBP^{OG} protein (measured at the 8 h time point) was lower than in nuclear extracts from refed and glucose force-fed mice. (Fig. 2*D*), and as a consequence *L-PK* was not induced (Fig. 2*E*). Our results suggest that ChREBP stabilization by *O*-GlcNAcylation does not lead to an active protein in the absence of an active glucose flux.

The role of *O*-GlcNAcylation on ChREBP stability was further addressed in hepatocytes (Supplementary Fig. 2). Global *O*-GlcNAcylation levels were enhanced in 5 mmol/L GlcNH$_2$ or in G25i conditions. Incubation with MG132 led to a marked increase in ubiquitinylated proteins (Supplementary Fig. 2*B*). Under G5 conditions, MG132 raised ChREBP content to comparable levels to that in G25i conditions. Under GlcNH$_2$ conditions, ChREBP content was also increased to comparable levels to that in G25i conditions, but independently of MG132 addition. The MG132-mediated increase in ChREBP content was the result of a stabilization of the protein, since ChREBP mRNA levels remained low. *L-PK* expression was only induced under G25i conditions (Supplementary Fig. 2*C*).

To determine whether ChREBP was regulated by ubiquitinylation, ChREBP^{wt} was cotransfected in HEK293T cells with an ubiquitin-tagged HA vector (Ubi-HA) to allow the detection of ubiquitinylated forms. Addition of MG132 induced the stabilization of ubiquitinylated proteins as well as ubiquitinylated forms of ChREBP^{wt}, as revealed by the anti-HA antibody (Supplementary Fig. 2*D*). Our results show that ChREBP is ubiquitinylated after addition of MG132 and suggest that the *O*-GlcNAcylation stabilizes the ChREBP protein.

Hepatic OGT overexpression increases ChREBP transcriptional activity in fed mice. To address the functional consequences of raising ChREBP^{OG} in vivo, OGT overexpression was achieved in the liver of C57BL/6J mice (Fig. 3). OGT expression was increased by two- to threefold, leading to a rise in global *O*-GlcNAcylation levels (Fig. 3*A*). As a consequence, ChREBP protein content was increased, regardless of the nutritional status (Fig. 3*A*). ChREBP^{OG} was increased in the livers of refed versus fasted mice and was further increased in the OGT mouse liver (Fig. 3*C*). The OGT-mediated increase in ChREBP content was linked to a posttranslational stabilization of the protein because ChREBP mRNA levels were not modified (Fig. 3*B*). Interestingly, ChREBP^{OG} content was only increased in nuclear extracts from refed OGT mice but not in the livers of fasted OGT mice (Fig. 3*D*). This difference was most likely due to the lack of increase in hepatic G6P concentrations in the livers of fasted OGT mice (Supplementary Table 1).

shown). *D*: Detection of nuclear ChREBP^{OG} by WGA binding in nuclear extracts from 24-h fasted, refed, and/or force-fed mice with either glucose (5 *g/kg*) or GlcNH$_2$ (2.5 *g/kg*) for 8 h. A representative Western blot is shown. *n* = 6–10 per group. Lanes were run on the same gel but were noncontiguous. *E*: Quantitative RT-PCR analysis of ChREBP (*blacks bars*) and L-PK (*white bars*) in the livers of the four groups of mice. Data are means ± SEM. *n* = 6–10 per group. *P < 0.01, **P < 0.005 compared with fasted mice (within the same color). (A high-quality digital representation of this figure is available in the online issue.)
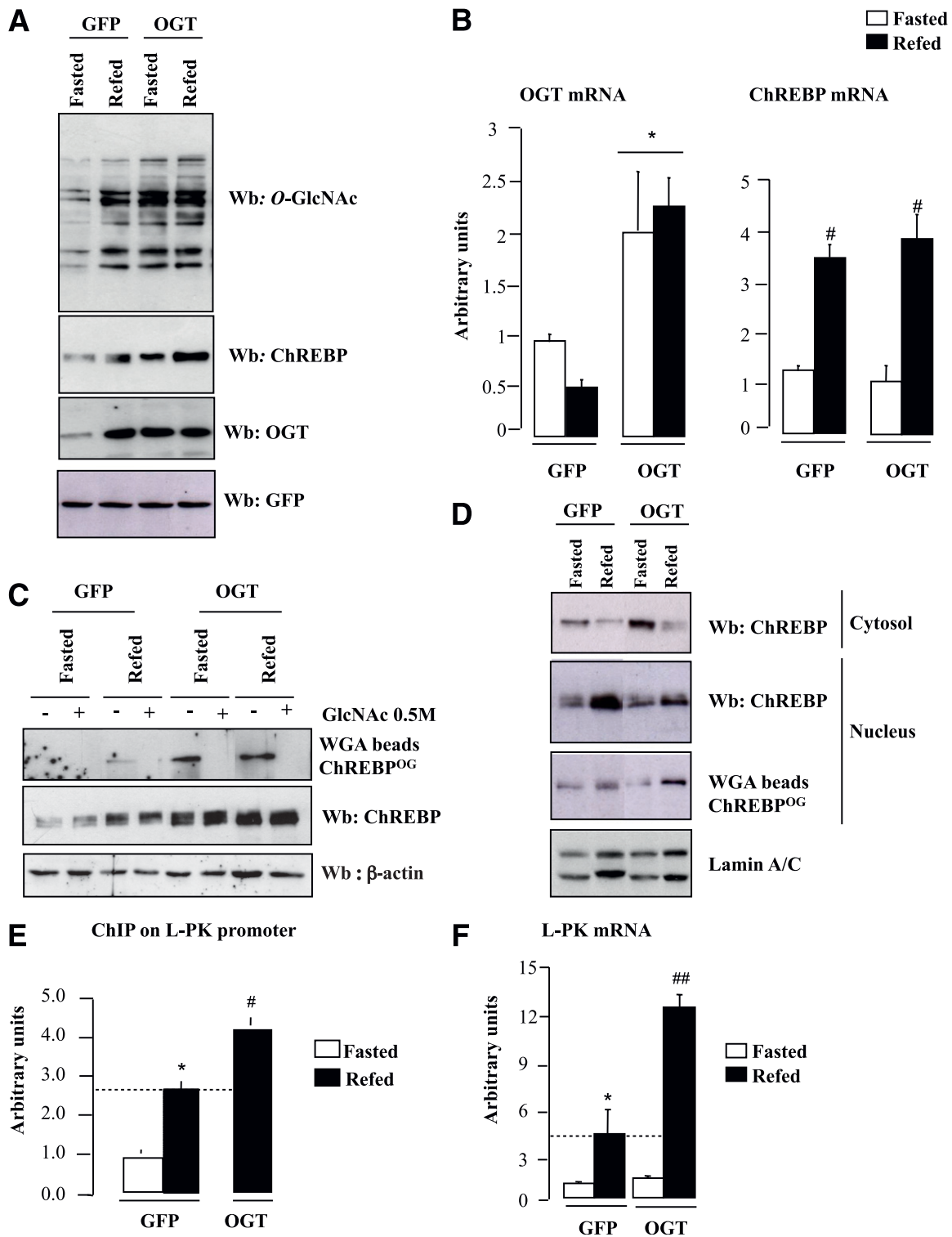
FIG. 3. OGT overexpression increases ChREBP protein content and activity in the liver of C57BL/6J mice. OGT (5×10^9 pfu/mouse) was over-expressed in the liver of C57BL/6J mice through penis vein injection. An equivalent dose of GFP adenovirus was used as control. Mice were fasted for 24 h or refed a regular diet following the fasting period ($n = 6$–10 mice per group). *A*: Liver extracts were immunoblotted with *O*-GlcNAc, ChREBP, and OGT antibodies. GFP was used as loading control. Representative Western blots (Wb) are shown. *B*: Quantitative RT-PCR analysis of OGT and ChREBP. Data are means ± SEM. $n = 6$ per group. *$P < 0.01$, OGT vs. GFP mice; #$P < 0.01$, refed vs. fasted. *C*: ChREBP^{OG} were obtained by WGA binding experiments. Specificity of the binding was confirmed by GlcNAc (0.5 mmol/L) competition. β-Actin was used as a loading control. Lanes were run on the same gel but were noncontiguous. *D*: ChREBP levels (cytosolic and nuclear) and nuclear ChREBP^{OG} were analyzed by Western blot. Lamin A/C was used as a control. Representative Western blots are shown. Lanes were run on the same gel but were noncontiguous. *E*: ChREBP at the ChoRE containing region of the *L-PK* promoter were measured by ChIP analysis. Immunoprecipitated *L-PK* promoter sequence was analyzed by quantitative PCR. Data are means ± SEM. $n = 3$ per group. *$P < 0.01$ compared with fasted GFP mice; #$P < 0.01$ compared with refed GFP mice. *F*: Quantitative RT-PCR analysis of *L-PK*. Data are means ± SEM. $n = 6$ per group. *$P < 0.01$ compared with fasted GFP mice; ##$P < 0.005$ compared with refed GFP mice. (A high-quality color representation of this figure is available in the online issue.)

Because Ser-196 is a key determinant of ChREBP cellular localization in response to glucose (8), *O*-GlcNAcylation of the ChREBP[DP] was measured in HEK293T cells (Supplementary Fig. 3). No significant difference in *O*-GlcNAcylation was observed between ChREBP[DP] and ChREBP[wt], suggesting that phosphorylation and *O*-GlcNAc modification(s) do not competitively occur on these sites. In agreement with this observation, translocation of ChREBP to the nucleus in response to refeeding was not affected under OGT conditions (Fig. 3*D*).

We next determined the importance of *O*-GlcNAcylation on ChREBP transcriptional activity. ChIP analysis revealed a 60% increased in ChREBP recruitment to the *L-PK* promoter in the liver of refed OGT mice (Fig. 3*E*). As a consequence, *L-PK* expression was significantly stimulated (Fig. 3*F*). To confirm the contribution of *O*-GlcNAcylation to ChREBP activity, luciferase activity of a *L-PK* reporter construct (25) was measured in HepG2 cells cotransfected with ChREBP[wt] (27) (Supplementary Fig. 4). A 12-fold increase in *L-PK* luciferase activity was measured under G25 conditions compared with G5. Addition of PUGNAc (5 μM), an inhibitor of the OGA, which hydrolyses the sugar (Fig. 1*A*), led to a further induction (30%), revealing that ChREBP[OG] plays part in its transcriptional activity (Supplementary Fig. 4).

Development of hepatic steatosis in OGT-overexpressing mice. We next determined the effects of OGT overexpression on glucose and lipid metabolism. A three- to fivefold increase in *ACC*, *FAS*, and *SCD1* gene expression was measured in refed GFP mice—an increase that was significantly potentiated in the liver of refed OGT mice (Fig. 4*A*). TG concentrations (Supplementary Table 1) as well as the number of lipid droplets stained with Oil Red O were markedly increased in the livers of refed OGT mice (Fig. 4*B*). Interestingly, lipogenic gene expression was not induced in the livers of fasted OGT mice and remained as low as in GFP fasted mice (Fig. 4*A*). This lack of induction was linked to the lack of concomitant increase in G6P concentrations (Supplementary Table 1) and in nuclear ChREBP[OG] in fasted OGT mice (Fig. 3*D*). OGT mice also exhibited increased fasting blood glucose (Supplementary Table 1 and Fig. 4*C*) as well as a moderate but significant glucose and insulin intolerance compared with GFP mice (Fig. 4*C*). These metabolic alterations were associated with elevated hepatic glucose-6-phosphatase (G6Pase) mRNA levels (Fig. 4*D*). This effect was likely due to increased CRTC2 *O*-GlcNAcylation (Fig. 4*E*), as previously shown (11). However, it should not be excluded that the effect observed on G6Pase could be directly linked to ChREBP[OG], since G6Pase gene expression is stimulated by glucose and that two ChoRE were identified on its promoter (28).

Lastly, because lipogenic gene expression is under the synergistic action of ChREBP and SREBP-1c (29), mRNA levels, precursor, mature forms, and *O*-GlcNAcylation of SREBP-1c were measured (Supplementary Fig. 5). No significant modification of SREBP-1c was observed upon OGT overexpression, suggesting a lack of SREBP-1c involvement in the OGT-mediated induction of lipogenic genes.

Overexpression and silencing of OGT in primary mouse hepatocytes. We next determined whether the OGT-mediated induction of lipogenic gene expression was strictly dependent on ChREBP (Fig. 5). As we observed in vivo (Fig. 3*A* and *C*), a threefold increased in OGT expression raised global *O*-GlcNAcylation levels and increased ChREBP total protein content in primary mouse hepatocytes (Fig. 5*A* and *B*). Under G25i conditions, *L-PK*,

FAS, and *SCD1* gene expression was further increased in OGT-overexpressing hepatocytes compared with GFP cells. Interestingly, the stimulatory effect of OGT was lost when ChREBP was silenced through a shRNA strategy (Fig. 5*B* and *C*). The effect was the result of ChREBP deficiency. Indeed, under OGT+shChREBP conditions, ChREBP protein content was markedly decreased compared to OGT overexpression and returned to levels nearly comparable to GFP conditions (Fig. 5*B*). SREBP-1c expression remained unchanged under the culture conditions tested (Fig. 5*C*).

To confirm the importance of modulating OGT activity for ChREBP protein content and/or activity, OGT expression was silenced through a shRNA approach in mouse hepatocytes (Fig. 6). ChREBP[OG] was significantly reduced compared with control conditions when OGT expression was knocked-down under G25i conditions (Fig. 6*A* and *B*). Total ChREBP protein content was also markedly reduced (Fig. 6*A*), independently of a decrease in ChREBP mRNA levels (Fig. 6*C*). This observation is in agreement with a destabilization effect of deglycosylated ChREBP protein. Importantly, under shOGT conditions, ChREBP-target gene expression (*L-PK*, *ACC*, *FAS*, and *SCD1*) was significantly decreased (Fig. 6*C*).

Altogether, our in vivo and in vitro results (Figs. 3–6) demonstrate that modulating OGT activity (overexpression/ inhibition) affects glycolytic and lipogenic gene expression through ChREBP[OG].

OGA overexpression improves hepatic steatosis and the lipidic profile of *db/db* mice. Having determined that *O*-GlcNAcylation increases ChREBP activity under refed conditions and leads to excessive hepatic TG deposition (Figs. 3 and 4), we determined, as a complementary experiment, whether deglycosylation of ChREBP could improve hepatic steatosis and related metabolic alterations in obese mice. To this purpose, we chose to overexpress the OGA enzyme through an adenoviral approach (24) in the livers of *db/db* mice, rather than silencing OGT (Fig. 6), in order to address the relevance of the OGT/OGA balance for ChREBP activity and function in the liver (Fig. 7). First, we observed that ChREBP[OG] was increased in the liver of GFP-*db/db* mice (compared with GFP controls) and was correlated to increased ACC and FAS protein content (Fig. 7*D*), elevated TG concentrations (Fig. 7*E*), steatosis (Fig. 7*C*), and hyperglycemia (Supplementary Table 2) in these mice. Ten days after OGA delivery, a moderate increase in OGA expression was detected, in agreement with the observation that OGA overexpression peak is achieved 3 days after adenoviral injection (Fig. 7*A*) (30). Nevertheless, significant physiological and metabolic modifications were observed; OGA-*db/db* mice showed decreased fasting blood glucose and improved glucose tolerance compared with GFP-*db/db* mice (Supplementary Table 2 and Fig. 7*B*)—metabolic improvements that were associated with a decrease in the *O*-GlcNAcylation of CRTC2 (Fig. 7*D*), a key coactivator involved in the control of hepatic glucose production (11). Interestingly, OGA overexpression also significantly reduced ChREBP[OG] levels (Fig. 7*D*), a decrease that was associated with diminished ACC and FAS protein content (Fig. 7*D*) and improved hepatic steatosis (Fig. 7*C*). Histological analysis of liver sections from OGA-*db/db* mice revealed a marked decrease in lipid droplets size and number, as revealed by Oil Red O staining (Fig. 7*C*). Supporting these observations, liver and plasma TG levels were significantly decreased (Fig. 7*E*). ChREBP total protein content was also decreased in the liver of OGA-*db/db* mice (Fig. 7*D*), likely as a result of a destabilization of
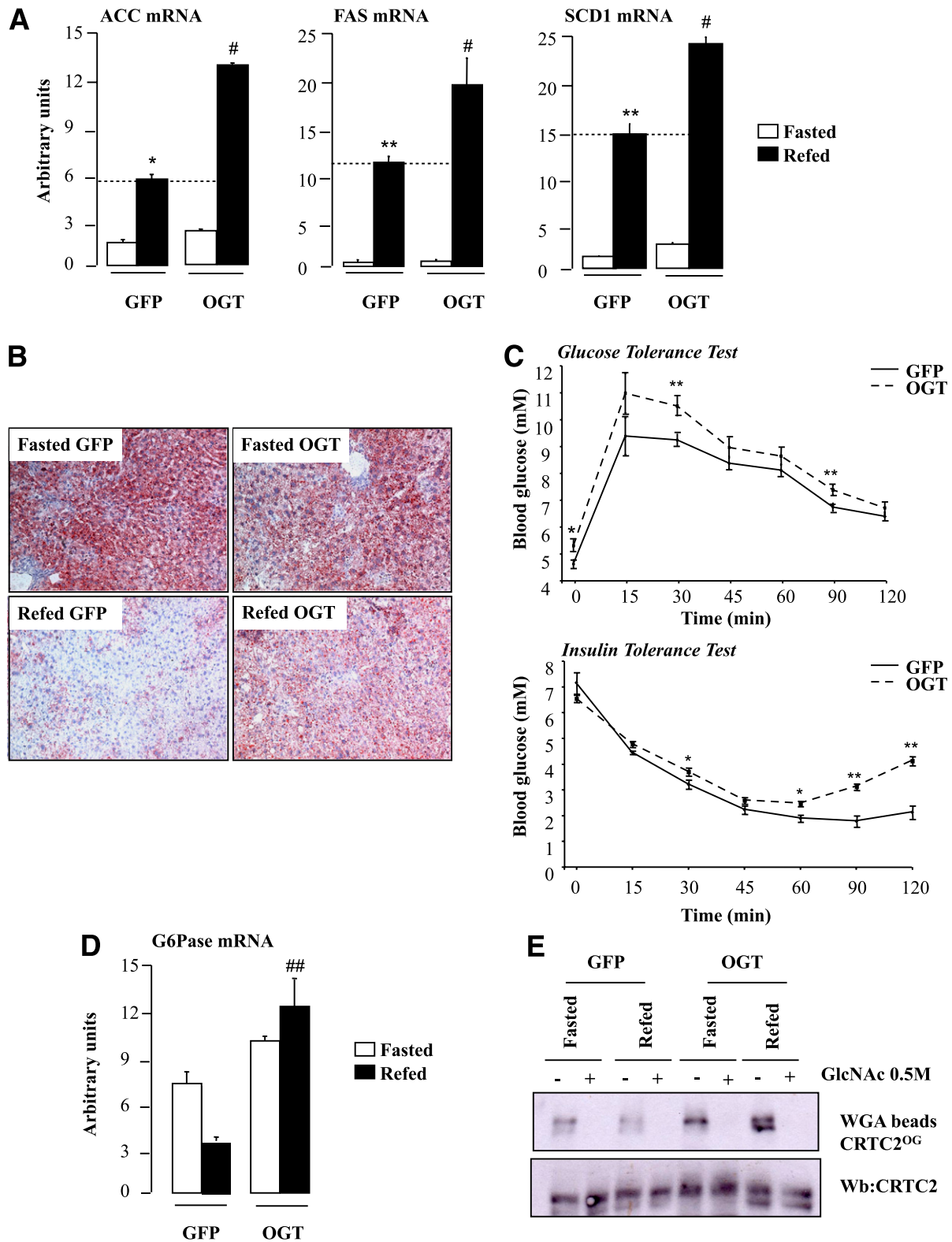
FIG. 4. ChREBP[OG]-mediated induction of the lipogenic program in the liver of OGT mice. *A*: Quantitative RT-PCR analysis of *ACC*, *FAS*, and *SCD1*. Data are means ± SEM. $n = 6$ per group. *$P < 0.01$; **$P < 0.005$ compared with fasted GFP mice; #$P < 0.005$ compared with refed GFP mice. *B*: Oil Red O staining of liver sections from GFP and OGT mice (original magnification ×20). *C*: Glucose tolerance (1 g/kg) and insulin tolerance (0.75 units/kg) tests were performed in GFP and OGT mice. Data are means ± SEM. $n = 6$–10 mice per group. *$P < 0.01$; **$P < 0.005$ compared with GFP mice. *D*: Quantitative RT-PCR analysis of G6Pase. Data are means ± SE. $n = 6$ per group. ##$P < 0.005$ compared with refed GFP mice. *E*: CRTC2[OG] were obtained by WGA binding. Specificity of the binding was confirmed by GlcNAc (0.5 mmol/L) competition. Representative Western blots (Wb) of *O*-GlcNAcylated and total CRTC2 forms are shown. (A high-quality digital representation of this figure is available in the online issue.)
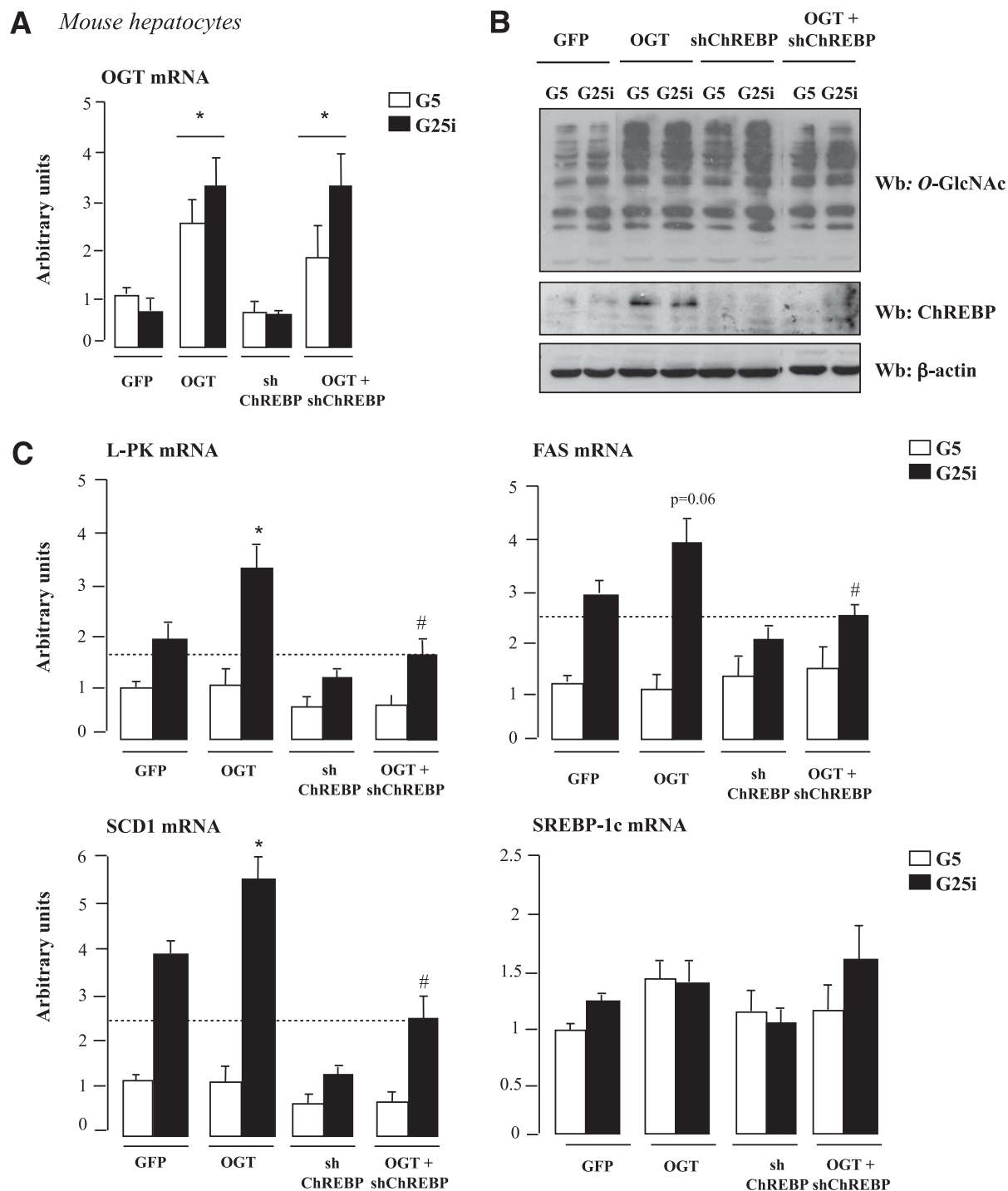
A *Mouse hepatocytes*

FIG. 5. The stimulatory effect of OGT on lipogenic gene expression is lost when ChREBP is silenced. Mouse hepatocytes were incubated under low glucose concentrations (G5) and adeno-infected with 5 plaque-forming units/cell of GFP, OGT, shChREBP, or OGT+shChREBP adenovirus for 5 h. Cells were then incubated for 24 h under low glucose (G5) or high glucose concentrations plus insulin (G25i). *A*: Quantitative RT-PCR analysis of OGT. Data are means ± SEM. $n = 6$ independent cultures. $*P < 0.05$ compared with GFP. *B*: Global *O*-GlcNAcylation levels and ChREBP protein content. β-Actin was used as a loading control. Representative Western blots (Wb) are shown. $n = 6$ independent experiments. Lanes were run on the same gel but were noncontiguous. *C*: Quantitative RT-PCR analysis of *L-PK, FAS, SCD1*, and *SREBP-1c*. $*P < 0.05$ compared with GFP (G25i); $\#P < 0.05$ compared with OGT (G25i). Data are means ± SEM. $n = 6$ independent cultures.

the deglycosylated ChREBP protein. This effect was specific, since total CRTC2 protein content was not affected by OGA treatment (Fig. 7D).

Taken together, our results reveal that increased ChREBP[OG] is correlated to hyperglycemia and steatosis in *db/db* mice and that hepatic OGA overexpression, by affecting ChREBP activity (*O*-GlcNAcylation and content),

significantly improved the lipidic profile and decreased hepatic steatosis of *db/db* mice.

Deglycosylation of ChREBP reduces lipid droplet accumulation in hepatocytes. To confirm the direct consequence of modulating ChREBP[OG] via OGA on lipid synthesis, OGA was overexpressed in hepatocytes (Fig. 8A). OGA overexpression led to significant reduction in

A *Mouse hepatocytes*

B

ChREBP^{OG}/Total ChREBP
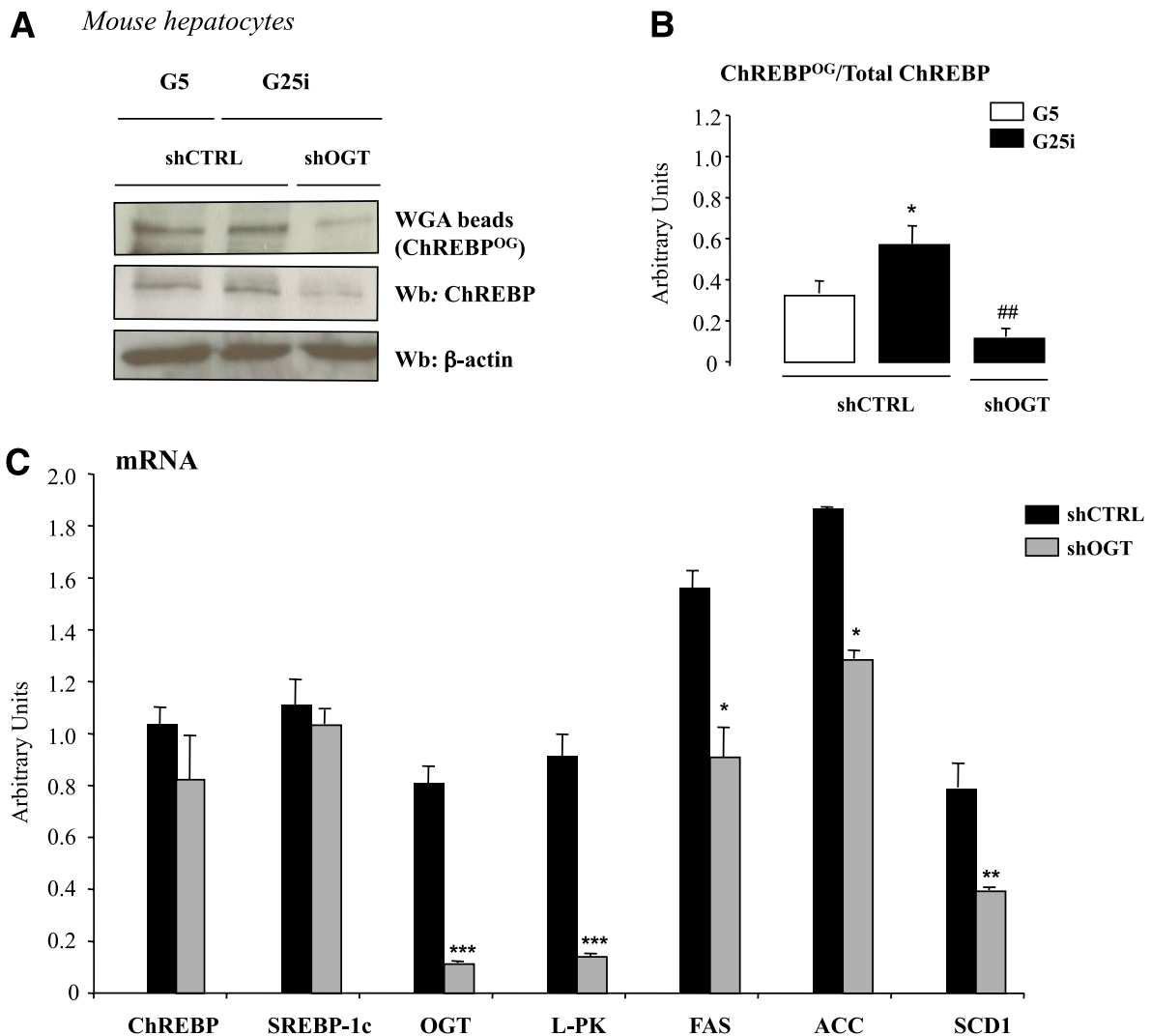
C

mRNA

FIG. 6. OGT silencing decreases ChREBP^{OG} levels and ChREBP-target gene expression in primary mouse hepatocytes. Mouse hepatocytes were incubated under low glucose concentrations (G5) and adeno-infected with 5 pfu/cell of control (shCTRL) or shOGT adenovirus for 5h. Cells were then incubated for 24 h under low glucose (G5) or high glucose concentrations plus insulin (G25i). *A*: ChREBP^{OG} were obtained by WGA binding. Representative Western blots (Wb) of *O*-GlcNAcylated and total ChREBP protein are shown. $n = 5$ independent cultures. *B*: Quantification of the ratio of ChREBP^{OG} compared with total ChREBP content is shown. Data are means ± SEM. $n = 5$ independent cultures. *$P < 0.05$ compared with G5 conditions; ##$P < 0.01$ compared with shCTRL conditions (G25i). *C*: Quantitative RT-PCR analysis of ChREBP, SREBP-1c, OGT, L-PK, ACC, FAS, and SCD1. *$P < 0.01$; **$P < 0.005$; ***$P < 0.001$ compared with shCTRL (G25i). Data are means ± SEM. $n = 5$ independent cultures. (A high-quality color representation of this figure is available in the online issue.)

both global and ChREBP^{OG} (Fig. 8*B*). ChREBP mRNA concentrations were not affected, confirming that OGA only affects ChREBP at the posttranslational level (Fig. 8*C*). Surprisingly, in contrast to long-term OGA treatment in vivo (10 days, Fig. 7), short-term OGA overexpression in vitro (48 h) did not affect ChREBP total protein content (Fig. 8*B*). As a direct consequence of decreased ChREBP^{OG}, *L-PK*, *ACC*, and *SCD1* expression was significantly reduced (Fig. 8*C*), leading to a visible decrease in lipid droplet accumulation after Oil Red O staining under G25i conditions (Fig. 8*D*). Altogether, our results show that decreasing ChREBP^{OG} affects its activity and prevents lipid accumulation in primary hepatocytes.

DISCUSSION

Over the recent years, ChREBP has emerged as a central regulator of lipid synthesis in the liver through the transcriptional control of glycolytic and lipogenic gene expression in response to glucose (2,8,31). The fact that liver-specific inhibition of ChREBP improves hepatic steatosis in obese *ob/ob* mice (5) prompted us to provide a better knowledge of the regulation of its activity in the liver. So far, phosphorylation had been the only posttranslational modification described to modulate ChREBP activity (7,9). Interestingly, recent work from our laboratory revealed that ChREBP is regulated by acetylation on specific lysines in response to glucose (31). In the current study, we report that ChREBP is also subjected to *O*-GlcNAcylation; *O*-GlcNAcylation not only stabilizes the protein but also increases its transcriptional activity toward its target genes (*L-PK*, *ACC*, *FAS*, and *SCD1*) when combined with an active glucose flux in vivo. More importantly, our results suggest that *O*-GlcNAcylation increases ChREBP activity under hyperglycemic conditions and therefore leads to excessive TG deposition in the liver.

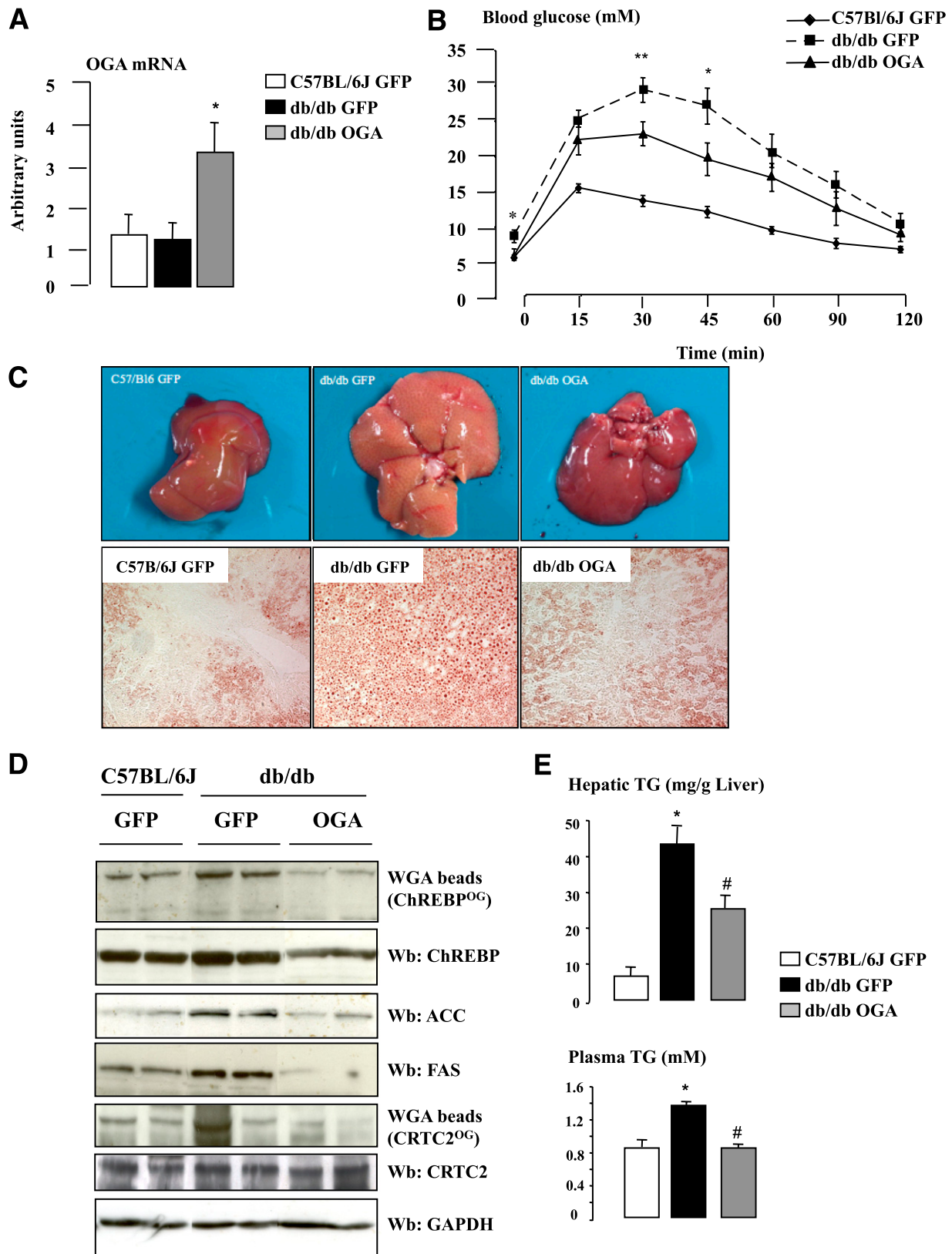Several transcription factors are modified by *O*-GlcNAcylation (10,15). This posttranslational modification

FIG. 7. Hepatic steatosis is improved in *db/db* mice overexpressing OGA. OGA (5×10^9 pfu/mouse) was overexpressed in the liver of *db/db* mice through penis vein injection. An equivalent dose of GFP adenovirus was injected to C57BL/6J and to another group of *db/db* mice. Mice were studied at the fed state. $n = 5$–6 mice per group. *A*: Quantitative RT-PCR analysis of OGA. *$P < 0.05$ compared with GFP mice. *B*: Glucose tolerance (1 g/kg) tests were performed in GFP- and OGA-treated mice. Data are means ± SEM. $n = 5$–6 mice per group. *$P < 0.01$; **$P < 0.005$ compared with GFP-*db/db* mice. *C*: Hepatic steatosis is prevented in OGA-*db/db* mice. Oil Red O staining of liver sections from GFP-C7BL/6J, GFP-*db/db*, and OGA-*db/db* mice (original magnification ×20). *D*: ChREBP^{OG} and CRTC2^{OG} levels, and ChREBP, ACC, FAS, and CRTC2 total protein content. GAPDH was used as a loading control. Representative Western blots (Wb) are shown. Lanes were run on the same gel but were noncontiguous. *E*: Liver and plasma TG concentrations. *$P < 0.01$ compared with GFP-C57BL/6J mice; #$P < 0.01$ compared with GFP-*db/db* mice. (A high-quality digital representation of this figure is available in the online issue.)
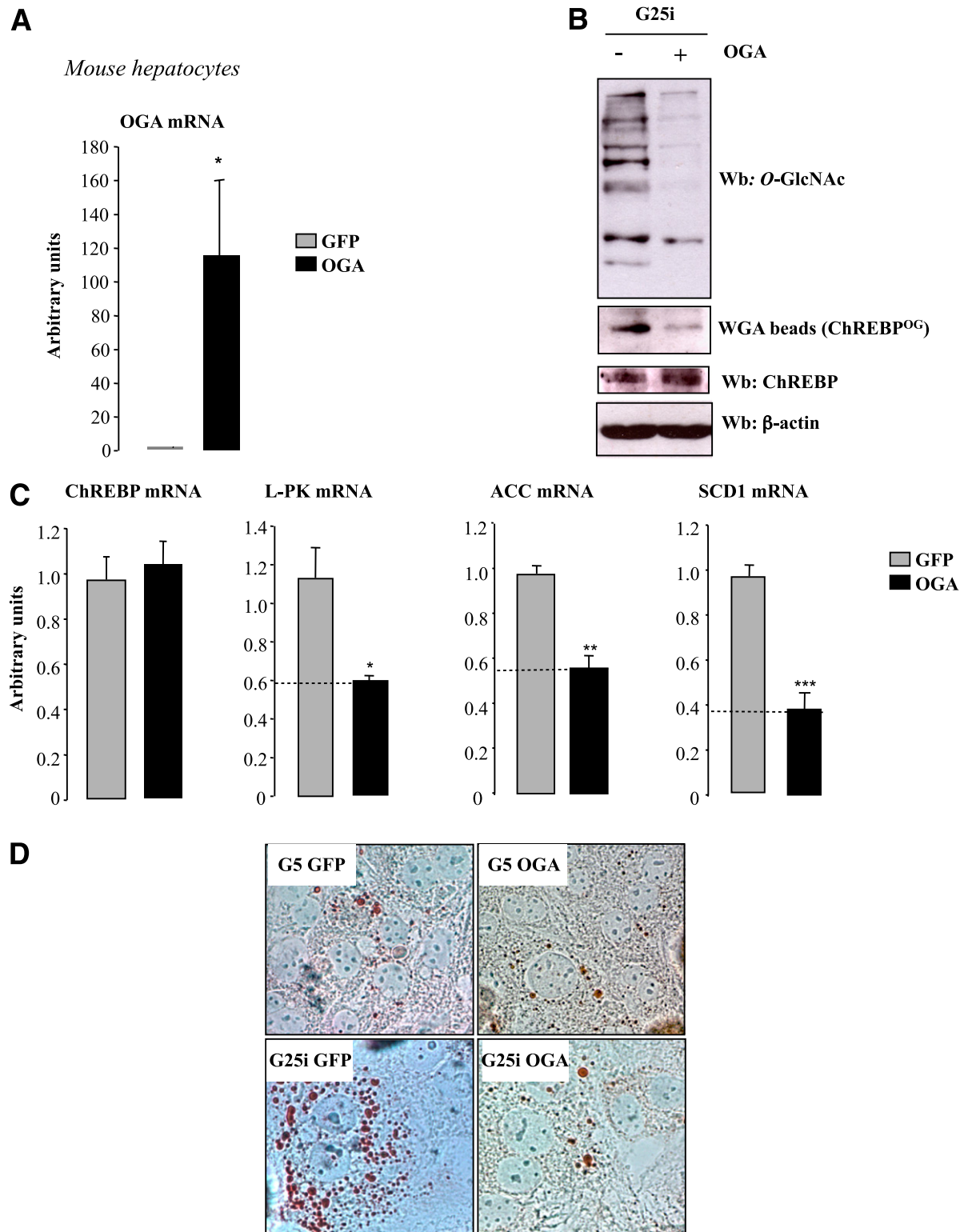
FIG. 8. OGA overexpression in vitro leads to ChREBP deglycosylation and decreased lipid droplet accumulation. Primary mouse hepatocytes were incubated under low glucose concentrations (G5) and adeno-infected with either 5 pfu/cell of GFP or OGA adenovirus for 5 h. Cells were then incubated 24 h with high glucose concentrations plus insulin (G25i). *A*: Quantitative RT-PCR analysis of OGA. Data are means ± SEM. $n = 4$ independent cultures. *$P < 0.005$ compared with GFP. *B*: Global and specific ChREBP^{OG}. β-Actin was used as a loading control. Representative Western blots (Wb) are shown. $n = 4$ independent experiments. *C*: Quantitative RT-PCR analysis of *ChREBP, L-PK, ACC,* and *SCD1*. *$P < 0.05$; **$P < 0.01$; ***$P < 0.005$ compared with GFP. Data are means ± SEM. $n = 4$ independent cultures. *D*: Oil Red O staining of hepatocytes infected with either 5 pfu/cell of GFP or OGA adenovirus (original magnification ×40). (A high-quality digital representation of this figure is available in the online issue.)

has been proposed to act as a nutrient sensor because the donor sugar, UDP-GlcNAc, receives input from multiple metabolic pathways and the activity of OGT, the enzyme that transfers the monosaccharide to serine/threonine residues, depends upon UDP-GlcNAc concentrations (20) (Fig. 1*A*). *O*-GlcNAcylation regulates transactivation by altering recruitment of transcriptional machinery, DNA binding, nuclear localization, and/or protein stability (20,32). Sustained increase in *O*-GlcNAc levels has been implicated as a pathogenic contributor to glucose toxicity and insulin resistance, major hallmarks of type 2 diabetes and diabetes-related cardiovascular complications (33). Our study demonstrates a direct interaction between ChREBP and OGT in HEK293T cells and in hepatocytes. The fact that the interaction was stronger under low glucose concentrations suggests that ChREBP^{OG} may explain the residual ChREBP content under low glucose availability. This mechanism could lead to high ChREBP protein levels ready to be activated when glucose flux rapidly increases upon refeeding. Our results reveal that *O*-GlcNAcylation affects ChREBP protein stability, increasing ChREBP protein content independently of a stimulation of its transcription. Although previously reported as a rather labile protein, with an estimated half-life of 30 min (34), no study previously reported, to our knowledge, the mechanism(s) by which the ChREBP protein undergoes degradation in the liver. Our study reveals that ChREBP is ubiquitinylated and probably undergoes degradation through the proteasome, since MG132 treatment resulted in ChREBP protein stabilization under low glucose concentrations. Similar protein content was reached when hepatocytes were incubated with 5 mM GlcNH$_2$, indicating that ChREBP was stabilized by *O*-GlcNAcylation and protected against proteasomal degradation (Supplementary Fig. 6). This is also in agreement with the fact that proteasome function is inhibited by *O*-GlcNAc (35). Interestingly, when OGA was overexpressed in the liver of *db/db* mice, ChREBP total protein content was decreased, most likely through a specific destabilization of the deglycosylated ChREBP protein. In addition, the decrease in blood glucose concentrations observed upon OGA treatment in *db/db* mice (Supplementary Table 2) may have also contributed to reduce ChREBP content and/or *O*-GlcNAcylation. The fact that OGT silencing in vitro also affected total ChREBP protein concentrations (Fig. 6), supports the hypothesis that *O*-GlcNAcylation modulates ChREBP protein stability.

O-GlcNAcylation can also regulate the cellular localization of transcription factors (22). Nuclear translocation is a central determinant of ChREBP activity in response to glucose. It was demonstrated that ChREBP is translocated into the nucleus in response to high glucose concentrations (34). It was thus hypothesized that glucose flux through the pentose phosphate pathway promoted the formation of xylulose-5-phosphate, which then activated the protein phosphatase 2A, which dephosphorylates Ser-196, a cAMP-dependent protein kinase target residue, located near the nuclear localization signal domain and promotes ChREBP nuclear translocation (7). Although alternate mechanisms were proposed to explain the glucose-mediated activation of ChREBP (36), we reported that modulation of Ser-196 phosphorylation was a key determinant of ChREBP cellular localization (8). Under fed conditions, ChREBP is nuclear and dephosphorylated on Ser-196, whereas after a bolus of glucagon, which actives cAMP-dependent protein kinase activity and mimics a fasting state, ChREBP phosphorylation on Ser-196 is increased and the transcription factor is exported from the nucleus to the cytoplasm. The current study reports that ChREBP^{OG} does not affect its cellular localization. Under fasting conditions, GlcNH$_2$ treatment, or OGT overexpression, ChREBP protein content is increased but ChREBP nuclear localization is not modified, suggesting that a signal dependent on glucose metabolism is still needed for its translocation. When OGT is expressed in the liver of fasted mice, only a low fraction of ChREBP^{OG} is detected in liver nuclear extracts, suggesting that under low glucose availability *O*-GlcNAcylation stabilizes the ChREBP protein but does not allow its nuclear translocation. The fact that *O*-GlcNAcylation of the ChREBP^{DP} was not reduced compared with the one of ChREBP^{wt} suggests that *O*-GlcNAcylation and phosphorylation do not competitively occupy these particular sites, and that Ser-196, which is important for ChREBP nuclear translocation, is still accessible to dephosphorylation when ChREBP is *O*-GlcNAcylated. The identification of the specific *O*-GlcNAcylation residues within the ChREBP protein will be important in the future to determine their specific contribution to ChREBP transcriptional activity and/or modulation of stability.

Glucose responsiveness of ChREBP is not only dependent on its nuclear localization but also on its ability to bind the ChoRE present in the promoter of its target genes. It was previously proposed that Thr-666 dephosphorylation promotes ChREBP DNA binding and transcriptional activation (34). However, the fact that mutation of this site does not result in a constitutively active ChREBP isoform (9) confirms that the regulation of ChREBP activity in response to glucose is complex and may involve multiple posttranslational modifications (31) and/or intramolecular regulations (36,37) like it is the case for other transcription factors such as FoxO1 whose regulation involves phosphorylation, acetylation, ubiquitination, and/or *O*-GlcNAcylation (10). In the current study, we show that ChREBP^{OG} increases its recruitment to the L-PK ChoRE under OGT overexpression conditions as well as its transcriptional activity toward the *L-PK* gene in HepG2 cells. When ChREBP^{OG} occurred in the context of an active glucose flux, a potentiating effect on *L-PK* and lipogenic gene expression was observed. While *ACC*, *FAS*, and *SCD1* genes were described as synergistically regulated by ChREBP and SREBP-1c (29), we report here that the stimulatory effect of OGT on lipogenic genes is highly dependent on ChREBP activity (Fig. 5). In addition, the fact that SREBP-1c *O*-GlcNAcylation was not modified by OGT overexpression strongly argues for a ChREBP-dependent effect.

Lastly, our results suggest that *O*-GlcNAcylation may contribute to increased ChREBP content under hyperglycemic conditions (i.e., in the livers of obese mice) and may lead to excessive hepatic TG deposition. Accumulation of TG within hepatocytes is the hallmark of nonalcoholic fatty liver disease, an increasingly common health concern that encompasses a spectrum of hepatic pathology, ranging from simple steatosis, to steatohepatitis, fibrosis, and cirrhosis (38). Understanding the molecular steps involved in TG accumulation in the liver is important, as it may provide potential therapeutic targets for the treatment and prevention of nonalcoholic fatty liver disease. Our results suggest that *O*-GlcNAcylation may represent an important modulator of ChREBP activity and could contribute, by stabilizing and stimulating ChREBP transcriptional activity, to the phenotype of hepatic steatosis in obese mice (Fig. 7). Accordingly, modulation of ChREBP^{OG} in the liver of OGT mice led to the development of hepatic steatosis,

whereas OGA overexpression in vivo by decreasing ChREBP content/*O*-GlcNAcylation markedly reduced TG concentrations in the livers of *db/db* mice and improved their lipidic phenotype. It should be noted that the effects we observed on whole glucose homeostasis and insulin sensitivity upon OGT and/or OGA modulation were also linked to the modification of CRTC2 *O*-GlcNAcylation and/or of protein(s) of the insulin signaling pathway, as previously reported (11,24). Nevertheless, our results emphasize the importance of ChREBP in the control of hepatic fatty acid synthesis and reveal that *O*-GlcNAcylation represents a novel regulation of ChREBP protein content and activity in the liver under both physiological and pathophysiological conditions.

REFERENCES

1. Postic C, Girard J. Contribution of de novo fatty acid synthesis to hepatic steatosis and insulin resistance: lessons from genetically engineered mice. J Clin Invest 2008;118:829–838
2. Dentin R, Pégorier JP, Benhamed F, et al. Hepatic glucokinase is required for the synergistic action of ChREBP and SREBP-1c on glycolytic and lipogenic gene expression. J Biol Chem 2004;279:20314–20326
3. Ishii S, Iizuka K, Miller BC, Uyeda K. Carbohydrate response element binding protein directly promotes lipogenic enzyme gene transcription. Proc Natl Acad Sci U S A 2004;101:15597-15602
4. Ma L, Tsatsos NG, Towle HC. Direct role of ChREBP.Mlx in regulating hepatic glucose-responsive genes. J Biol Chem 2005;280:12019–12027
5. Dentin R, Benhamed F, Hainault I, et al. Liver-specific inhibition of ChREBP improves hepatic steatosis and insulin resistance in ob/ob mice. Diabetes 2006;55:2159–2170
6. Iizuka K, Miller B, Uyeda K. Deficiency of carbohydrate-activated transcription factor ChREBP prevents obesity and improves plasma glucose control in leptin-deficient (ob/ob) mice. Am J Physiol Endocrinol Metab 2006;291:E358–E364
7. Kabashima T, Kawaguchi T, Wadzinski BE, Uyeda K. Xylulose 5-phosphate mediates glucose-induced lipogenesis by xylulose 5-phosphate-activated protein phosphatase in rat liver. Proc Natl Acad Sci USA 2003;100:5107–5112
8. Denechaud PD, Bossard P, Lobaccaro JM, et al. ChREBP, but not LXRs, is required for the induction of glucose-regulated genes in mouse liver. J Clin Invest 2008;118:956–964
9. Tsatsos NG, Towle HC. Glucose activation of ChREBP in hepatocytes occurs via a two-step mechanism. Biochem Biophys Res Commun 2006;340:449–456
10. Issad T, Kuo M. O-GlcNAc modification of transcription factors, glucose sensing and glucotoxicity. Trends Endocrinol Metab 2008;19:380–389
11. Dentin R, Hedrick S, Xie J, Yates J 3rd, Montminy M. Hepatic glucose sensing via the CREB coactivator CRTC2. Science 2008;319:1402–1405
12. Housley MP, Rodgers JT, Udeshi ND, et al. O-GlcNAc regulates FoxO activation in response to glucose. J Biol Chem 2008;283:16283–16292
13. Housley MP, Udeshi ND, Rodgers JT, et al. A PGC-1alpha-O-GlcNAc transferase complex regulates FoxO transcription factor activity in response to glucose. J Biol Chem 2009;284:5148–5157
14. Anthonisen EH, Berven L, Holm S, Nygård M, Nebb HI, Grønning-Wang LM. Nuclear receptor liver X receptor is O-GlcNAc-modified in response to glucose. J Biol Chem 2010;285:1607–1615
15. Ozcan S, Andrali SS, Cantrell JE. Modulation of transcription factor function by O-GlcNAc modification. Biochim Biophys Acta 2010;1799:353–364
16. Puigserver P, Rhee J, Donovan J, et al. Insulin-regulated hepatic gluconeogenesis through FOXO1-PGC-1alpha interaction. Nature 2003;423:550–555
17. Koo SH, Flechner L, Qi L, et al. The CREB coactivator TORC2 is a key regulator of fasting glucose metabolism. Nature 2005;437:1109–1111
18. Kuo M, Zilberfarb V, Gangneux N, Christeff N, Issad T. O-glycosylation of FoxO1 increases its transcriptional activity towards the glucose 6-phosphatase gene. FEBS Lett 2008;582:829–834
19. Zeidan Q, Hart GW. The intersections between O-GlcNAcylation and phosphorylation: implications for multiple signaling pathways. J Cell Sci 2010;123:13–22
20. Hart GW, Housley MP, Slawson C. Cycling of O-linked beta-N-acetyl-glucosamine on nucleocytoplasmic proteins. Nature 2007;446:1017–1022
21. Love DC, Hanover JA. The hexosamine signaling pathway: deciphering the "O-GlcNAc code". Sci STKE 2005;2005:re13
22. Guinez C, Morelle W, Michalski JC, Lefebvre T. O-GlcNAc glycosylation: a signal for the nuclear transport of cytosolic proteins? Int J Biochem Cell Biol 2005;37:765–774
23. Marshall S, Garvey WT, Traxinger RR. New insights into the metabolic regulation of insulin action and insulin resistance: role of glucose and amino acids. FASEB J 1991;5:3031–3036
24. Yang X, Ongusaha PP, Miles PD, et al. Phosphoinositide signalling links O-GlcNAc transferase to insulin resistance. Nature 2008;451:964–969
25. Lou DQ, Tannour M, Selig L, Thomas D, Kahn A, Vasseur-Cognet M. Chicken ovalbumin upstream promoter-transcription factor II, a new partner of the glucose response element of the L-type pyruvate kinase gene, acts as an inhibitor of the glucose response. J Biol Chem 1999;274:28385–28394
26. Green H, Kehinde O. An established preadipose cell line and its differentiation in culture. II. Factors affecting the adipose conversion. Cell 1975;5:19–27
27. Stoeckman AK, Ma L, Towle HC. Mlx is the functional heteromeric partner of the carbohydrate response element-binding protein in glucose regulation of lipogenic enzyme genes. J Biol Chem 2004;279:15662–15669
28. Pedersen KB, Zhang P, Doumen C, et al. The promoter for the gene encoding the catalytic subunit of rat glucose-6-phosphatase contains two distinct glucose-responsive regions. Am J Physiol Endocrinol Metab 2007;292:E788–E801
29. Dentin R, Girard J, Postic C. Carbohydrate responsive element binding protein (ChREBP) and sterol regulatory element binding protein-1c (SREBP-1c): two key regulators of glucose metabolism and lipid synthesis in liver. Biochimie 2005;87:81–86
30. Soesanto YA, Luo B, Jones D, et al. Regulation of Akt signaling by O-GlcNAc in euglycemia. Am J Physiol Endocrinol Metab 2008;295:E974–E980
31. Bricambert J, Miranda J, Benhamed F, Girard J, Postic C, Dentin R. Salt-inducible kinase 2 links transcriptional coactivator p300 phosphorylation

to the prevention of ChREBP-dependent hepatic steatosis in mice. J Clin Invest 2010;120:4316–4331

32. Butkinaree C, Park K, Hart GW. O-linked beta-N-acetylglucosamine (O-GlcNAc): Extensive crosstalk with phosphorylation to regulate signaling and transcription in response to nutrients and stress. Biochim Biophys Acta 2010;1800:96–106

33. Karunakaran U, Jeoung NH. O-GlcNAc modification: friend or foe in diabetic cardiovascular disease. Korean Diabetes J 2010;34:211–219

34. Yamashita H, Takenoshita M, Sakurai M, et al. A glucose-responsive transcription factor that regulates carbohydrate metabolism in the liver. Proc Natl Acad Sci USA 2001;98:9116–9121

35. Zhang F, Su K, Yang X, Bowe DB, Paterson AJ, Kudlow JE. O-GlcNAc modification is an endogenous inhibitor of the proteasome. Cell 2003;115: 715–725

36. Li MV, Chen W, Harmancey RN, et al. Glucose-6-phosphate mediates activation of the carbohydrate responsive binding protein (ChREBP). Biochem Biophys Res Commun 2010;395:395–400

37. Li MV, Chang B, Imamura M, Poungvarin N, Chan L. Glucose-dependent transcriptional regulation by an evolutionarily conserved glucose-sensing module. Diabetes 2006;55:1179–1189

38. Jou J, Choi SS, Diehl AM. Mechanisms of disease progression in nonalcoholic fatty liver disease. Semin Liver Dis 2008;28:370–379